Toughening Polylactide with Graft-Block Polymers

Bongjoon Lee[†], Michael J. Maher[†], Haley J. Schibur[†], Marc A. Hillmyer[‡,*], Frank S. Bates[†,*]

[†]Department of Chemical Engineering and Materials Science and [‡]Department of Chemistry, University of Minnesota, Minneapolis, MN 55455-0431

Abstract

Poly[(styrene-*alt*-N-hydroxyethylmaleimide)-*ran*-(styrene-*alt*-N-ethylmaleimide)]-*graft*-[poly(4-methylcaprolactone)-*block*-poly((±) -lactide)] (g-ML) graft polymers containing 50 vol% poly((±)-lactide) (PLA), were mixed with a commercial PLA homopolymer to modify the brittle mechanical behavior of this industrially compostable plastic. Various graft architectures, including linear, tri-arm and tetra-arm polymer backbones, were prepared using a grafting-from method. Small-angle X-ray scattering (SAXS) and transmission electron microscopy (TEM) revealed that the pure g-MLs form a lamellar morphology where the degree of long-range order is dictated by the polymer architecture. When melt-blended with PLA at low concentrations the g-MLs formed well-dispersed nanoscale particles within the PLA matrix, yielding moldable plastics with high optical transparency. The tensile toughness of the PLA/g-ML blends was substantially enhanced over that of pure PLA using g-ML concentrations as low as 5 wt% and exhibited average strains at break of 280% following 2 days of aging at room temperature; pure PLA failed at 7% strain. The elastic modulus, yield stress and transparency of the toughened plastic were virtually unaffected by the low concentration of rubbery poly(4-methylcaprolactone) (M) domains and the formation of well-dispersed nanoscale particles. Graft block polymers were shown to toughen PLA more efficiently than a linear triblock copolymer analogue LML, which produced a strain at break of 105 % at a loading of 5 wt%. Blending g-ML into PLA significantly delays the onset of physical aging and the onset of the ductile-to-brittle (DTB) transition, which depends on the concentration of g-ML utilized.

Keywords: *sustainable polymers, polymer toughening, graft polymer, polymer micelles, physical aging*

* Corresponding authors: hillmyer@umn.edu; bates001@umn.edu

Table of contents graphic

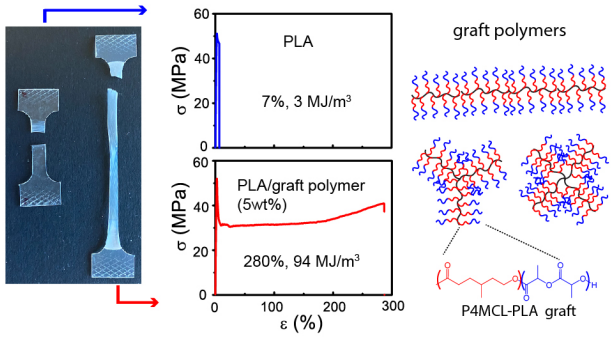

1. Introduction

Due to lightweight, low cost and exceptional mechanical properties, plastics are found in grocery bags, diapers, cell phones, household plumbing, automobile components, and many other common products. Most plastics are derived from non-renewable sources such as petroleum and natural gas, and are non-degradable, which contributes to environmental pollution.[1] For example, many synthetic plastics are discarded after single use, which results in landfill waste or pollution in the oceans, and do not substantively degrade over decades. In comparison, polylactide (PLA) can be derived from renewable sources and is susceptible to hydrolytic degradation and industrial composting rendering it more environmentally sustainable than most petroleum-based polymers.[1–4] PLA is a high modulus plastic and is produced at economically competitive prices relative to petroleum-based plastics.[5] However, the inherent brittleness and low impact strength of PLA present limitations to its wider implementation.[6]

Various strategies, including copolymerization, plasticization, and melt blending with rubber have been employed to toughen PLA.[7–9] Combining PLA with certain rubbery materials can provide control of the dispersion and morphology of rubbery domains at the nanoscale. Such dispersed rubbery domains function as stress concentrators due to their low modulus compared to the matrix and facilitate rubber particle cavitation and matrix shear yielding.[10] Block copolymers (BCPs) of PLA and soft rubbery blocks including poly(β-methyl-γ-valerolactone)[11] and poly(γ-methyl-ε-caprolactone)[12] have been shown to improve mechanical properties. Such BCPs are often melt blended with homopolymers to achieve desirable properties at lower cost than pure BCPs.[11] Plasticization by melt miscible, low T_g, additives increases the flexibility and ductility of PLA chains by lowering the glass transition temperature. A number of plasticizers, including lactide monomer,[12] citrate esters,[13] poly(ethylene glycols),[14] poly(ethylene oxide)[15] and poly(vinyl

acetate),[16] have been studied and the elongation at break has been shown to increase dramatically with increasing concentration of the plasticizer. However, effective plasticization generally requires a relatively high concentration of additive, typically more than 10 wt%, resulting in a loss of tensile strength and a significant reduction in the glass transition temperature, which greatly limits applications.[8] Furthermore, low molar mass molecules that are typically used tend to migrate to the surface leading to contamination and embrittlement over time.[7,17]

Melt blending PLA with rubbery material is an economical and convenient approach to tune its properties.[9] A host of elastomeric polymers have been melt blended with PLA to improve toughness, including linear low-density polyethylene,[18] polycaprolactone,[19] poly(butylene adipate-co-terephthalate),[20] natural rubber[21], ethylene-propylene copolymer,[22] ethylene-acrylic rubber,[22] acrylonitrile-butadiene rubber[22] and poly(butylene succinate).[23] However, melt blending with rubber often results in micron-scale particles due to thermodynamic immiscibility, which reduces transparency and compromises the mechanical properties; addition of a block copolymer compatibilizer can reduce the surface tension between the rubber and PLA mitigating these effects.[8,24,25]

Pure block copolymers also have been shown to be effective additives for improving the toughness of PLA. Li *et al.* and McCutcheon *et al.* have demonstrated that low molar mass poly(ethylene oxide)-poly(butylene oxide) (PEO-PBO) diblock copolymers form well-dispersed particles in PLA, leading to a dramatic enhancement in tensile toughness and impact strength without sacrificing the elastic modulus and transparency of the material; however, the yield strength decreased significantly.[24,26] BCPs including poly(ethylene oxide)-poly(propylene oxide)-poly(ethylene oxide) (PEO-PPO-PEO)[27] and a multiblock copolymer of polycaprolactone-PLA[28]

also have been employed to toughen PLA, and BCPs have been employed to toughen other brittle polymers including polypropylene and polystyrene.[11,29,30]

We explored graft block polymers as alternative modifiers for toughening PLA. Improved mechanical and rheological properties of undiluted graft polymers, versus linear analogues, have been reported earlier.[31–34] The application of graft, and graft-block, polymers as additives to toughen brittle polymers has not received significant attention. A graft-block molecular architecture resembles tri-arm, tetra-arm, and higher functionality star-polymers, which have attractive processing characteristics, including low melt viscosities.[35,36] Moreover, star-shaped polycaprolactone has been shown to improve the tensile toughness and impact properties of PLA.[37,38]

Previously, we reported that undiluted graft-block polymers, poly[(styrene-*alt*-N-hydroxyethylmaleimide)-*ran*-(styrene-*alt*-N-ethylmaleimide)]-*graft*-[poly(4-methylcaprolactone)-*block*-poly(±-lactide)], containing 80–100% PLA forms a tough plastic.[34] These compounds, denoted g-ML, displayed superior mechanical properties over the linear counterpart (LML) and significantly retarded PLA aging kinetics.[34] Also, previous studies have shown that graft polymers can function as compatibilizers in polymer blends.[39,40] We speculated that these excellent mechanical properties, along with a large number of interfacial entanglements with the matrix, and relatively low melt viscosity, would make g-ML polymers good candidates for toughening brittle PLA. In addition, the mechanical and rheological properties of g-ML can be tuned by varying the length of the backbone, number of graft chains, grafting density and molar mass of the grafts.[33] In this study, g-MLs containing 50% by volume PLA are examined for toughening a commercially available PLA homopolymer. P4MCL (the M block) is also a degradable polymer with a low glass transition temperature, $T_{g,M} = –55$ °C.[41–43] The molecular architecture, number of grafts and molar

mass of the graft polymers were systematically varied and the influence of these structural characteristics on the morphology and mechanical property of the blends was established. We also report on the kinetics of physical aging of PLA/g-ML blends.

2. Materials and Methods

Experimental details of polymer synthesis, processing and characterization can be found in the Supporting Information.

3. Results and Discussion

3.1 Pure Triblock and Graft-block Copolymers

Graft polymers (g-MLs), poly[(styrene-*alt*-*N*-hydroxyethylmaleimide)-*stat*-(styrene-*alt*-ethylmaleimide)]-*graft*-[poly(4-methyl caprolactone)-*block*-poly(±-lactide)] with linear, tri-arm and tetra-arm backbone chains were synthesized using a grafting-from technique.[44] Representative ^{1}H-NMR spectra of g-MLs are shown in Figure S1. In addition to the linear backbone graft polymer reported by Maher *et al*.,[44] tri-arm and tetra-arm polymer backbones were synthesized in this study using 1,1-tris[(dodecylthiocarbonothioylthio)-2-methylpropionate]ethane and pentaerythritol tetrakis[2-(dodecylthiocarbonothioylthio)-2-methylpropionate] as RAFT agents, respectively (Scheme 1). Characterization data for the backbone polymers used to prepare g-MLs are summarized in Table S1. Subsequently, P4MCL and PLA blocks were sequentially grown by initiation of ring-opening transesterification polymerization (ROTEP) from the pendant hydroxyl groups resulting in graft-block polymers (g-MLs) with linear, tri-arm and tetra-arm backbone structures as shown in Scheme 2. The molar mass of the graft was fixed at approximately15 kDa with 50% by volume PLA. The molar mass of the PLA blocks is close to the entanglement molar

mass (8.7kg/mol) and the molar mass of P4MCL is above the entanglement molar mass (2.9kg/mol).[18,41,45] The molecular architecture of g-ML with a tri-arm or tetra-arm polymer backbone resembles that of star graft polymers.[36]

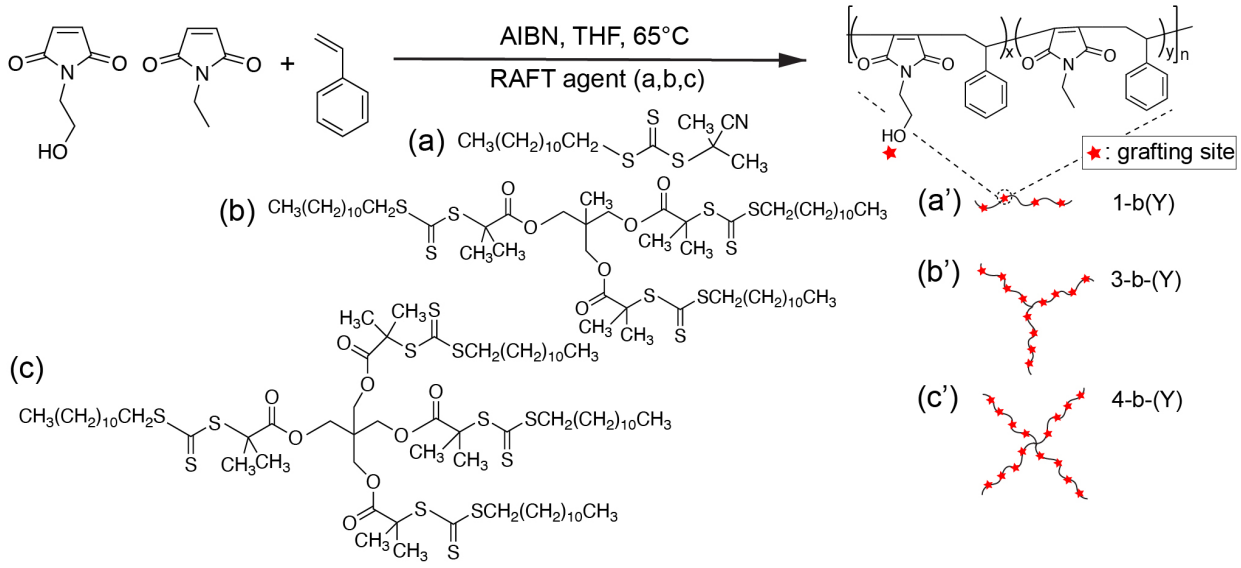

Scheme 1. Synthesis of linear, tri-arm and tetra-arm backbone polymers (a',b',c') using various RAFT agents (a,b,c). The number of grafting sites per arm (Y) varies from 10 to 40 for the linear g-MLs (a') and was fixed at 10 for tri-arm and tetra-arm g-MLs (b', c').

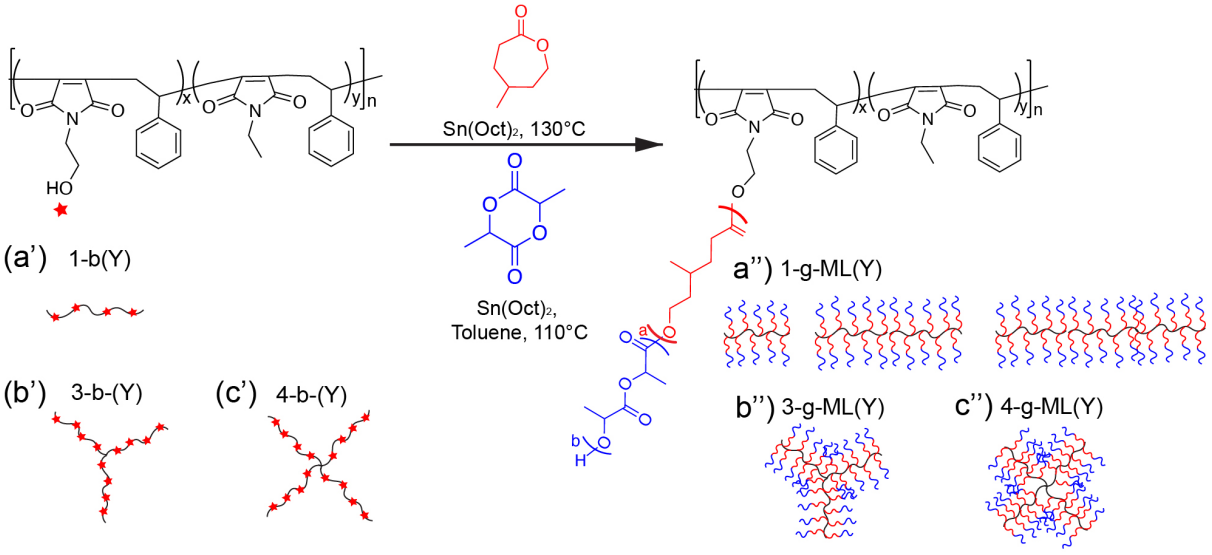

Scheme 2. Synthesis of g-MLs, poly[(styrene-*alt*-*N*-hydroxyethylmaleimide)-*stat*-(styrene-*alt*-ethylmaleimide)]-*graft*-[poly(4-methyl caprolactone)-*block*-poly(±-lactide)]. PLA and P4MCL blocks are grafted onto backbone polymers (a',b',c') to form linear, tri-arm and tetra-arm g-MLs

(a'',b'',c''), respectively. The number of grafts per arm (Y) varies from 10 to 40 for linear g-MLs (a'') and was fixed at 10 for tri-arm and tetra-arm g-MLs (b'', c'').

A linear triblock copolymer (LML) with the same composition as the g-MLs, 50 vol% PLA, was synthesized for comparison purposes using ring opening transesterification polymerization as reported by Watts *et al.*[41] The LML compound is analogous to g-ML with one backbone repeat unit and two grafts; the molar mass was chosen to match that of two grafts. Molecular characterization data for LML and the g-MLs are summarized in Table 1. In this report, the graft-block polymers are named X-g-ML(Y) where X denotes the number of arms per backbone (1 for linear, 3 for tri-arm and 4 for tetra-arm) and Y denotes the number of grafts per arm. The molar masses of the grafts for all g-MLs are comparable, and SEC traces for the backbone polymers, the g-MLs and the LML are presented in Figure S2. The nomenclature for the backbone polymers is X-b(Y) where X refers to the number of arms per backbone (1 for linear, 3 for tri-arm and 4 for tetra-arm) and Y indicates the number of grafting sites per arm.

Table 1. Characterization data for triblock and graft-block polymers containing 50% PLA by volume

Structure	Total Number of grafts	$M_{n,graft\ P4MCL}$[a] (kDa)	$M_{n,graft\ PLA}$[b] (kDa)	$M_{n,tot}$[c] (kDa)	$Đ$	f_{PLA}[d]	*% backbone*[e]
LML[f]	2	7.5	9.5	46	1.14	0.51	0
1-g-ML(10)	10	6.0	8.0	240	1.17	0.52	5.8
1-g-ML (30)	30	6.9	8.2	810	1.29	0.50	3.7
1-g-ML(40)	40	7.1	8.4	1,000	1.32	0.50	3.4
3-g-ML (10)	30	7.1	8.0	620	1.70	0.48	3.7

4-g-ML (10)	40	6.7	9.0	1,200	1.49	0.53	2.7

[a] Number average molecular weight (M_n), determined from % conversion by ^{1}H-NMR
[b] Number average molecular weight (M_n), determined by ^{1}H-NMR
[c] Determined by SEC-MALS (SEC-multi-angle light scattering with a THF mobile phase)
[d] Calculated assuming densities ρ_{P4MCL}=1.04g/mL and ρ_{PLA}=1.25g/mL at 25 °C. The backbone contribution is ignored.[34]
[e] % of the overall polymer mass associated with the backbone
[f] Triblock copolymer is analogous to a graft polymer with two grafts

Figure 1 shows differential scanning calorimetry data for the triblock and graft-block copolymers. All the polymers exhibit two glass transitions corresponding to P4MCL ($T_g \approx -53$ °C) and PLA ($T_g \approx 42$ °C) domains consistent with microphase separated morphologies.[41] The glass transition temperatures of all the polymers are listed in Table S2; all the values are comparable, attributable to the common molar mass of the grafts. Also, all the polymers exhibit nearly identical order-disorder transition temperatures (T_{ODT}s), which were established based on the point where the dynamic elastic modulus (G′) discontinuously drops while heating the material. Consistent with a previous report dealing with similar graft-block copolymers,[47] we find that T_{ODT} is relatively invariant to the molecular architecture at fixed graft composition and molecular weight as illustrated in Figure S3, where $T_{ODT} = 180 \pm 10$ °C.

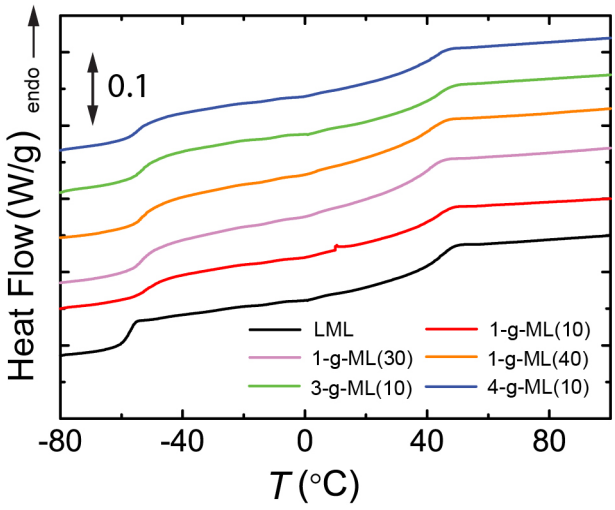

Figure 1. Differential scanning calorimetry curves of triblock copolymer (LML) and graft polymers (g-MLs) during 2nd heating at a rate of 10 °C/min. The DSC curves are vertically shifted for clarity. All the polymers show two glass transition temperatures associated with P4MCL ($T_g \approx -53$°C) and PLA ($T_g \approx 42$°C) consistent with microphase separation between the different blocks.

TEM images obtained from the pure triblock and graft-block copolymers are shown in Figure 2. All the polymers exhibit a lamellar morphology with various degrees of long-range order. LML displays large areas of uniform lamellar domains, while the lamellar domains of the g-MLs with 3 and 4 backbone branches are less homogeneous. SAXS patterns shown in Figure S4 are consistent with a reduction in long-range order with increasing molar mass (1-g-ML(10) versus 1-g-ML(30) versus 1-g-ML(40)) and backbone branching (3-g-ML(10) versus 4-g-ML(10)). The 4-g-ML(10) material shows more irregularities in lamellae spacing and more defects including interconnected lamellae structures. The lattice spacings deduced from the primary peak positions of SAXS patterns ($q^* = 0.026 - 0.032 Å^{-1}$) matches those measured from TEM images ($l = 20 \sim 24$ nm). Based on TEM and SAXS, we can conclude that the LML and g-ML materials display a lamellae morphology, which is moderately affected by the polymer architecture.

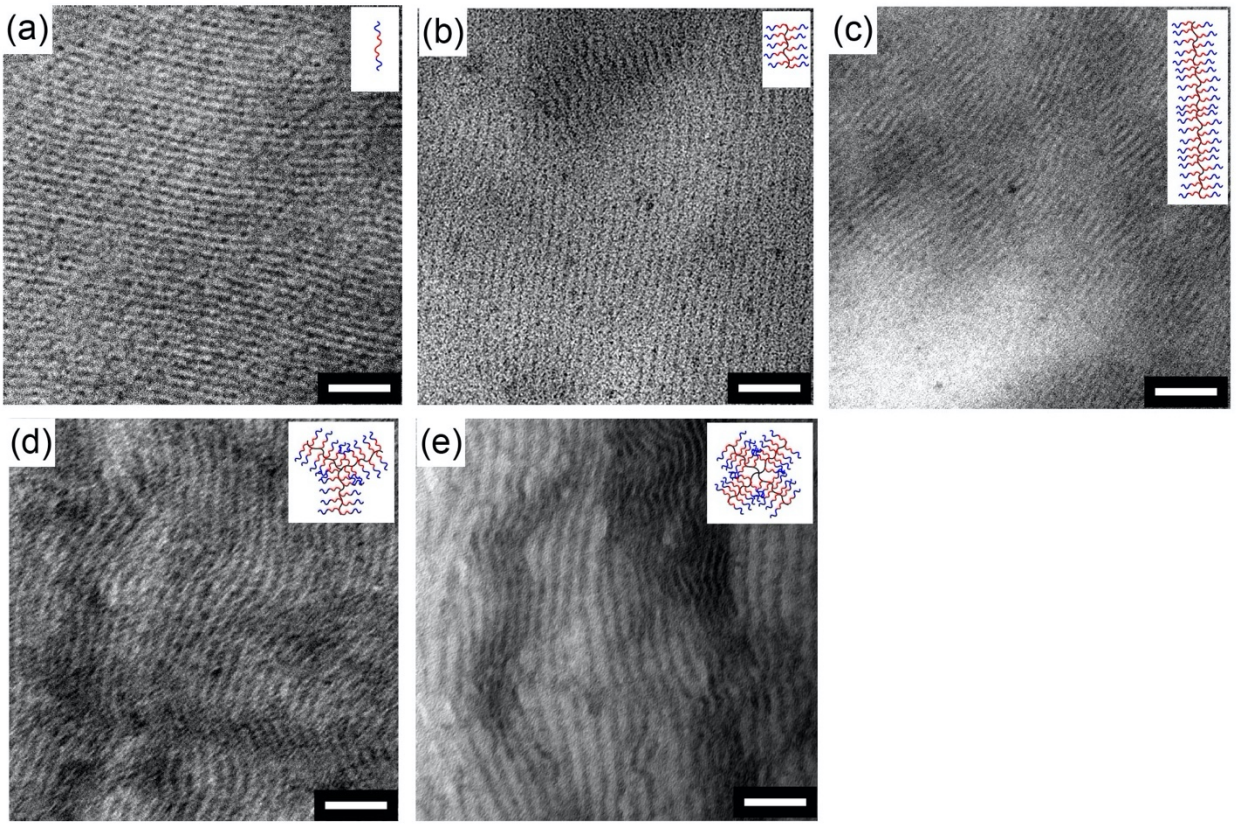

Figure 2. TEM images of (a) LML (b) 1-g-ML(10), (c) l-g-ML(40), (d) 3-g-ML(10), (e) 4-g-ML(10). Specimens were stained with RuO_4 which preferentially stains the P4MCL domains. The scale bars denote 100 nm.

The stress-strain behavior of the LML and g-MLs are shown in Figure 3. Both have similar elastic moduli and yield stresses as summarized in Table 2. Beyond the yield point, LML reaches a stress plateau, which extends to the point of failure, while all the g-MLs show significant strain hardening at $\varepsilon > 200\%$. All the copolymers are highly ductile with a strain at break of 450-500%. However, the g-MLs are characterized by a tensile strength $\sigma_b \approx 16$ MPa, which is roughly 50% greater than for LML. We attribute these results to the significantly higher number of intermolecular interactions associated with the graft-block copolymers versus the linear triblock copolymer.

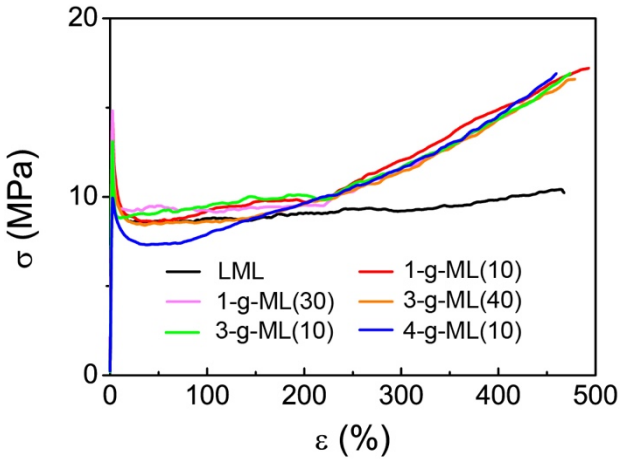

Figure 3. Stress-strain behavior of LML and g-MLs during tensile deformation at a strain rate of 10 mm/min. Graft-block polymers show significant strain hardening while LML exhibits a stress plateau. A complete set of stress-strain results are shown in Figure S5. Specimens were aged for 2 days prior to measurement.

Table 2. Mechanical properties of LML and g-MLs containing 50% PLA[a]

Name	***E* (MPa)**	**σ_y (MPa)**	***ε_y (%)***	**Toughness (MJ/m^3)**	**σ_b (MPa)**	***ε_b (%)***
LML	758±110	14±4	2.3+0.1	40±4	10+1	440±52
1-g-ML(10)	641±80	13±2	2.7+0.1	54±5	17±1	476±34
1-g-ML(30)	660±90	13±2	2.4±0.2	45±5	15±1	430±24
1-g-ML(40)	624±54	12±1	2.4±0.2	51±2	16±1	468±9
3-g-ML(10)	640±42	13±1	2.5±0.2	52±5	17±1	467±24
4-g-ML(10)	523±38	11±1	2.6±0.2	47±2	16±1	442±18

[a] Three or more measurements were averaged and the error denotes half the range of the data

3.2 PLA-Block Copolymer Blends

TEM images obtained from PLA blended with the LML and five g-MLs samples are shown in Figure 4. The concentration of block copolymer in the blends was fixed at 5 wt%. Since the composition of the LML and g-MLs polymers is approximately 50 vol% P4MCL, the total concentration of the rubbery P4MCL domains in the blends is only 2.5 wt% (≈ 3 vol%). All the LML and g-MLs are well dispersed in the PLA matrix due to the matrix compatible PLA blocks in the linear and graft block modifiers. The LML forms what appears to be a mixture of micelles and small aggregates, whereas g-ML, for example, 1-g-ML(10), forms particles with a layered structure with a spacing that matches that of the pure graft-blocks (see Figure 2 and Figure S6). The proposed molecular arrangement of LML and 1-g-ML(10) chains within the PLA matrix is shown in Figure 5. The interlayer spacing between layers is about 21 nm and agrees with SAXS data shown in Figure S7. SAXS patterns reveal a single broad peak at $q \cong 0.03$ Å^{-1} for the PLA/g-ML blends, however, PLA/LML blend shows a less distinct peak, consistent with the presence of fewer aggregated particles and more micelles. Multi-lamellar particles (i.e., vesicles) have been shown to produce a scattering peak that corresponds to the interlayer thickness.[46,47] All the blends display a relatively broad particle size distribution, and most of the particles appear to be elongated, which we interpret as being due to the flow of the material during the hot pressing procedure. The average particle size (corresponding to the minor axis in elongated particles) ranges between 65 and 105 nm and the particle size distributions for the blends are shown in Figure S8. Particle sizes associated with the PLA/g-ML blends are larger than those produced by the PLA/LML blend; for example, the average particle size for PLA/LML and PLA/3-g-ML(10) are 67 nm and 91 nm, respectively. This difference reflects a greater extent of g-ML association for the graft-block copolymers. Nevertheless, all 6 polymers are reasonably well dispersed in the PLA.

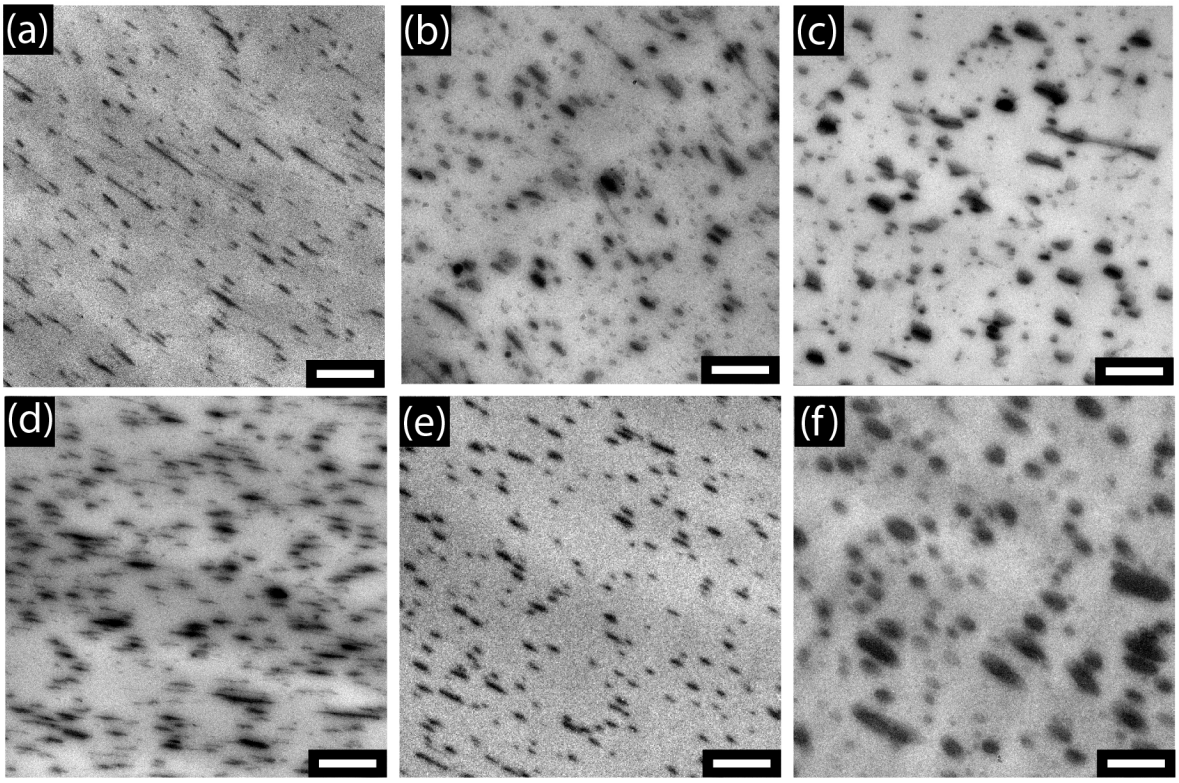

Figure 4. TEM images of PLA blended with 5 wt% of (a) LML, (b) 1-g-ML(10), (c) 1-g-ML(30), (d) 1-g-ML(40), (e) 3-g-ML(10) and (f) 4-g-ML(10). The scale bar represents 500 nm. TEM specimens were stained with RuO_4 to selectively darken the P4MCL domains. TEM images reveal formation of well-dispersed nanoparticles in the PLA matrix. Higher magnification TEM images are shown in Figure S6.

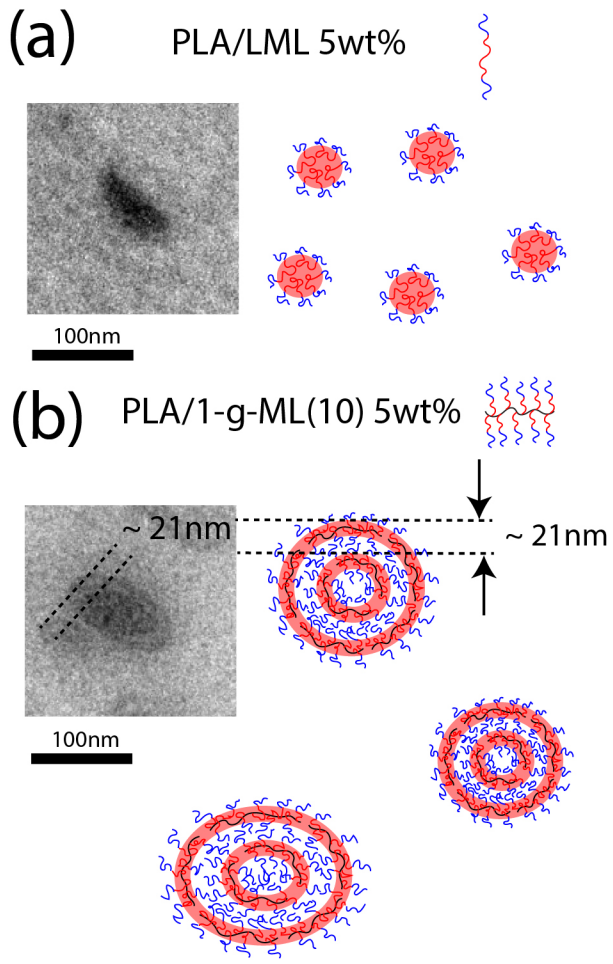

Figure 5. Postulated molecular arrangement of (a) LML and (b) 1-g-ML(10) polymer chains dispersed within the PLA matrix at 5 wt% concentration, based on TEM images shown. LML forms mostly polymer micelles whereas 1-g-ML(10) forms spherical bilayer vesicles with an interlayer spacing of 21 nm, consistent with the spacing derived from SAXS patterns shown in Figure S7.

PLA blends containing 5 wt% of the block copolymer additives exhibit high transparency as shown in Figure 6. This feature is highly desirable for many applications such as food packaging. Most rubber-toughened plastics are opaque due to the combination of large, i.e. micron size, particles and differences in refractive index between the matrix and rubbery phases.[24] The high transparency of the blends reported in this study is due to the combined effects of a low concentration of well dispersed nanoparticles (ca. 100 nm in size, Figure 5) with relatively modest

refractive index contrast between the matrix PLA and particles, which contain 50% by volume PLA.

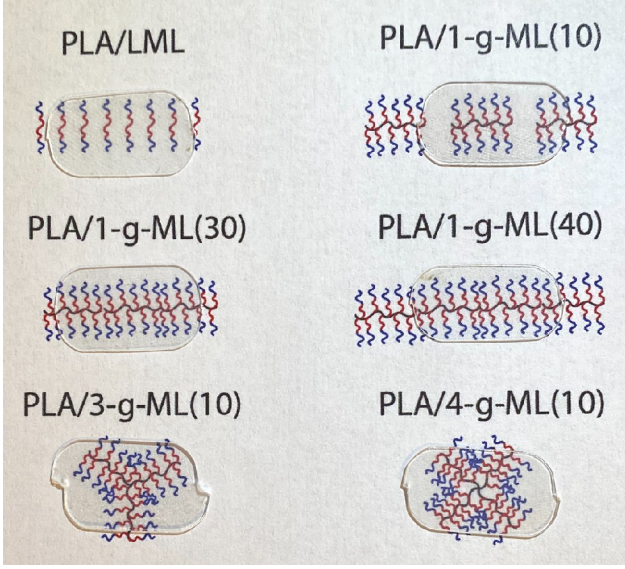

Figure 6. Optical image of films of PLA blended with 5 wt% of LML and the g-ML block copolymers demonstrating high transparency. Specimens were melt-blended at 180 °C for 10 minutes then hot pressed to obtain 0.2 mm thick sheets.

Representative stress-strain curves of blends prepared with LML and the g-MLs are shown in Figure 7; mechanical properties extracted from these data are tabulated in Table 3. Tensile specimens were aged for two days at room temperature prior to testing. The pristine PLA displays brittle failure, with strain at break of ε_b = 7%. Addition of to the LML increases ε_b to 105%, and blending the g-MLs further improves the tensile toughness where ε_b = 160 – 280 %. Based on the results from the 1-g-MLs, the tensile toughness appears to be dependent on the number of grafts. The elongation at break increases from 160% to 230% to 280% as the number of grafts increases from 10 to 30 and 40, respectively. 3-g-ML(10) and 4-g-ML(10) blended with PLA display elongations at break of 280% and 245%, respectively, which are indistinguishable within experimental error. A complete set of stress-strain results are shown in Figure S10. The impact of blending LML and g-ML on the elastic modulus and yield stress is insignificant as summarized in

Table 3, attributable to the small amount of rubbery P4MCL (2.5 wt%) present. However, this minor amount of rubbery polymer has a dramatic impact on the overall tensile toughness (area under the stress-strain curve) which increased 22 fold using LML and between 20 and 34 times for the g-MLs, relative to pure PLA. To the best of our knowledge, this represents the greatest enhancement in toughness of PLA reported in the literature at such low levels of added rubber, hence without sacrificing elastic modulus or yield stress. Several photographs of the PLA/3-g-ML(10) blend before and after tensile testing are shown in Figure S11. The patches of whitened gauge section of the tensile specimen indicate a mixture of plastic deformation, cavitation, and crazing.[48]

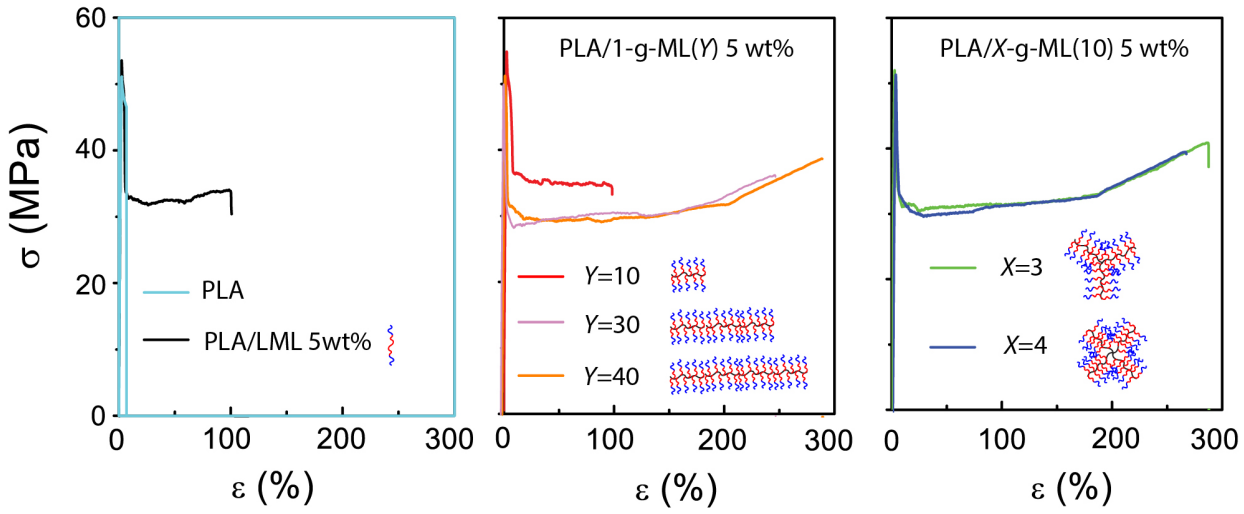

Figure 7. Stress-strain curve of: (left) pristine PLA, and PLA blended with LML; (middle) PLA blended with 1-g-ML(10), 1-g-ML(30), l-g-ML(40); (right) PLA blended with 3-g-BCP(10) and 4-g-ML(10). The concentration of modifiers (LML, g-MLs) is 5 wt% for all blends. The tensile toughness of PLA improves dramatically after blending with graft polymer modifiers. All tensile specimens were aged at room temperature for 2 days before testing and the strain rate was 1 mm/min. Stress-strain responses in the low strain (<10%) regime are shown in Figure S9.

Table 3. Mechanical properties of pristine PLA and PLA blended with 5 wt% of LML and g-MLs[a]

Name	***E* (GPa)**	**σ_y (MPa)**	***ε_y (%)***	**Toughness (MJ/m^3)**	**σ_b (MPa)**	***ε_b (%)***
PLA	2.5±0.1	53±2	2.6±0.1	2.8±1.1		6.7±2.5
PLA/LML	2.5±0.1	53±2	2.6±0.1	60±28	35±4	105±50
PLA/1-g-ML(10)	2.4±0.1	53±3	2.8±0.3	54±25	33±5	158±73
PLA/1-g-ML(30)	2.5±0.1	51±2	2.6±0.1	77±12	37±3	234±31
PLA/1-g-ML(40)	2.3±0.1	50±2	2.7±0.1	90±2	39±1	282±4
PLA/3-g-ML(10)	2.5±0.1	51±3	2.6±0.1	94±4	40±1	280±9
PLA/4-g-ML(10)	2.3±0.1	50±1	2.8±0.1	87±1	39±1	245±46

[a]At least three measurements were averaged, and the error denotes half the range of the data

The stress-strain curves of PLA blended with 2.5, 5, 10, and 20 wt% of 3-g-ML(10) are presented in Figure 8, and the associated tensile properties are tabulated in Table 4. Just 2.5 wt% of this graft-block copolymer increases the elongation at break from 7% to 83%. Increasing the concentration to 5 wt% yields ε_b = 280%, and this property remains essentially invariant up to 20 wt%. However, the plateau in the stress at higher strains drops above 5 wt% of 3-g-ML(10), which can be attributed to the greater rubber content and a much courser morphology as shown by TEM

images in Figure S12. Therefore, maximum toughness is obtained at about 5 wt% loading of the additive.

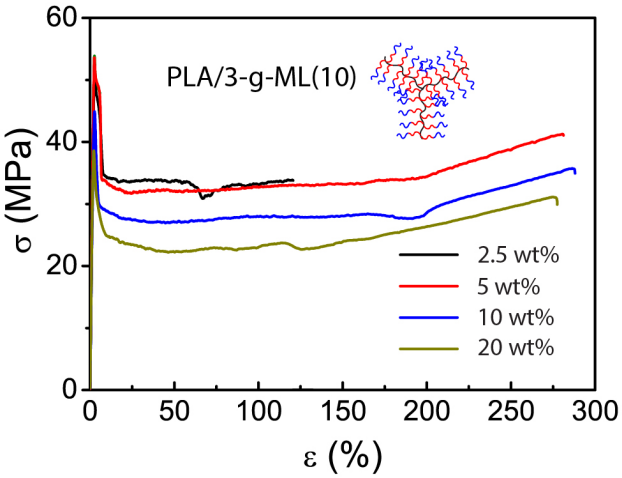

Figure 8. Stress-strain curves of PLA blended with 2.5 to 20 wt% of 3-g-ML. Tensile specimens were aged at room temperature for 2 days before testing at a strain rate of 1 mm/min.

Table 4. Mechanical properties of PLA blends with various concentration of 3-g-ML(10)

modifier concentration (wt%)	***E* (GPa)**	**σ_y (MPa)**	***ε_y (%)***	**Toughness (MJ/m^3)**	**σ_b (MPa)**	***ε_b (%)***
0	2.5±0.1	53±2	2.6±0.1	2.7±1.1		6.7±2.5
2.5	2.4±0.1	51±2	2.5±0.1	28±13	34±1	83±39
5	2.4±0.1	51±3	2.6±0.1	94±4	40±1	280±9
10	2.2±0.1	46±1	2.6±0.1	81±2	36±1	275±10
20	2.1±0.2	34±4	2.2±0.1	71±15	31±4	280±37

The TEM images, shown in Figure S12, also reveal the evolution of a coarser particle dispersion and more complex overall morphology with increasing concentrations of graft polymer.

At low concentration (2.5 wt%), the vesicles are smaller and form a single-layer. At high concentration (10, 20 wt%), the size distribution broadens, and the particle shapes are far from spherical. SAXS patterns shown in Figure S14 reveal that the internal spacing associated with block segregation remains the same at all concentrations. DSC measurements shown in Figure S13 demonstrate that the glass transition temperature of the PLA does not change with addition of up to 20 wt% 3-g-ML(10), consistent with segregation of the graft-block copolymer from the homopolymer matrix. It is worth noting that the blend maintains relatively high transparency while the concentration of g-ML in the blend increases from 2.5 to 20 wt% as shown in Figure S15. The stress-strain behavior of PLA blended with various concentration of 3-g-ML(10) during physical aging is shown in Figure 9. Tensile specimens were kept at room temperature for specified periods of time before testing. After aging 2 days, PLA/3-g-ML(10) (5wt%) blend shows ductile behavior with an elongation at break of 280%. However, after 15 days of aging, the elongation at break reduces to 125%, and the stress-strain curve begins to exhibit a double yield behavior as reported previously[26,49] with pristine g-ML containing 90% PLA.[34] After 22 days of aging, the 5 wt% blend material fails at about 22 % strain, before reaching the 2nd yield point. PLA blended with 5wt% of 1-g-ML(30) and 4-g-ML(10) also displayed a ductile to brittle transition (DBT) after 22 days of aging as shown in Figure S17.

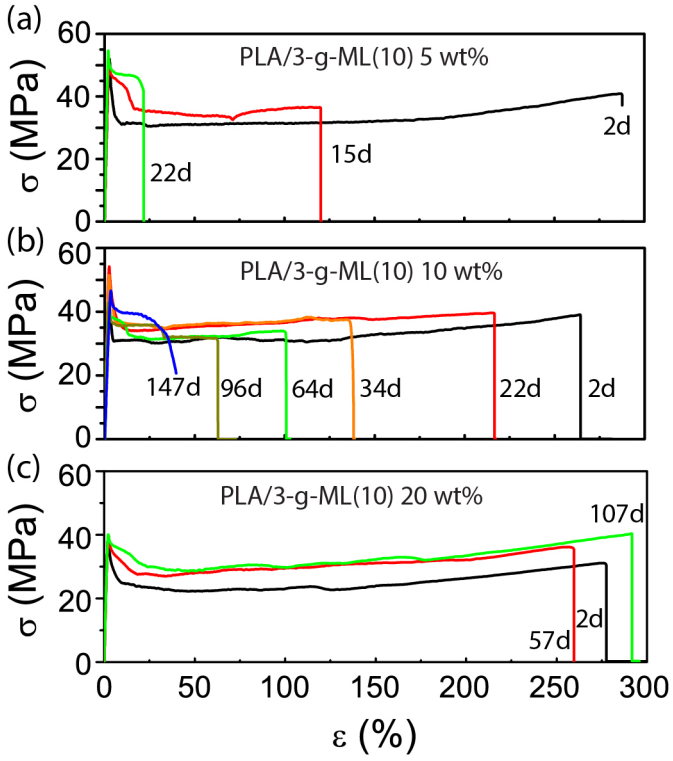

Figure 9. Stress-strain behavior of PLA blended with (a) 5 wt%, (b) 10 wt%, and (c) 20wt% of 3-g-ML(10) at various stages of physical aging at room temperature. During physical aging, the tensile specimen undergoes a ductile-to-brittle transition. The kinetics of physical aging are determined by the concentration of graft polymer in the blends. The low strain portions of these data are shown in Figure S16.

We previously showed that it took 21 days for pure 1-g-ML with 90 vol% PLA (10 vol% P4MCL) to undergo a DBT.[34] It is interesting to note that the same DBT time is realized in the PLA/3-g-ML(10) (5wt%) blend with only 2.5 wt% (3 vol%) of rubbery P4MCL. Surprisingly, adding a small amount of the graft-block copolymer to the commercial PLA homopolymer is more efficient at delaying aging than is the pure copolymer, and without reductions in the modulus and yield stress; the 1-g-ML with 90 vol% PLA (10 vol% P4MCL) was characterized by a 12.5% drop in elastic modulus and 15% reduction in the yield stress.[34] As the P4MCL content increases to 5wt% (10wt% of 3-g-ML(10)) in the PLA/3-g-ML(10) blend, the DBT is delayed to 147 days. For the

blend with 10 wt% of P4MCL (20wt% of 3-g-ML(10)), the tensile specimen did not show any sign of a decrease in elongation at break even after 107 days.

Conclusions

Blending graft-block copolymers containing 50% by volume rubbery P4MCL and 50% by volume PLA blocks, denoted g-MLs, with commercial PLA results in dramatic increases in toughness compared to the pristine brittle plastic. We have achieved the highest toughness, a 34-fold increase over pure PLA, by melt blending 5wt% of 3-g-ML(10), a 3-arm graft-block copolymer. Due to the low overall amount of rubbery P4MCL (2.5 wt.%) in the blend, the hardness and yield strength of the modified plastic were largely unaffected. The number of grafts and architecture of the g-ML modestly influence the toughness of the blends. These g-ML additives form well dispersed nanoparticles within a PLA matrix and the blends retain high optical transparency. The ductile to brittle transition (DBT), which occurs within about 1 day in pure PLA, can be delayed by more than 100 days by the addition of g-ML, where the kinetics of physical aging are determined by the concentration of the modifier.

Associated Content

Supporting Information

The Supporting Information is available free of charge.

Experimental details of polymer synthesis, processing and characterization; 1H-NMR spectra, SEC traces, glass transition temperatures and temperature dependent storage modulus of polymers; Characterization data of backbone polymers; SAXS traces and complete sets of stress-strain curves of polymers and PLA blends; Stress-strain curves of PLA blends in low strain (<10%)

regime; Low and high magnification TEM images of polymers and PLA blends ; Distribution of particle sizes in PLA blends; Photograph of PLA/3-g-ML(10) blend after tensile testing; DSC traces, photographs and stress-strain curves in low strain (<30%) regime of PLA blends with various concentrations of 3-g-ML(10); Stress-strain curves of PLA blends with l-g-ML(30) and 4-g-ML(10) during physical aging

Author Information

Corresponding Authors:
Marc A. Hillmyer – Department of Chemistry, University of Minnesota, Minneapolis, MN, 55455-0431, United States; orcid.org/0000-0001-8255-3853;
Email: hillmyer@umn.edu
Frank S. Bates – Department of Chemical Engineering and Materials Science, University of Minnesota, Minneapolis, MN, 55455-0132, United States; orcid.org/0000-0003-3977-1278;
Email: bates001@umn.edu

Co-Authors:
Bongjoon Lee – Department of Chemical Engineering and Materials Science, University of Minnesota, Minneapolis, MN, 55455-0132, United States
Email: bongjool@alumni.cmu.edu

Haley J. Schibur – Department of Chemical Engineering and Materials Science, University of Minnesota, Minneapolis, MN, 55455-0132, United States
Email: schib037@umn.edu

Michael J. Maher – Department of Chemical Engineering and Materials Science, University of Minnesota, Minneapolis, MN, 55455-0132, United States
Email: mjmaher@protonmail.com

Notes:

The authors declare no competing financial interest.

Acknowledgements

Support for this work was provided by the National Science Foundation (NSF) Center for Sustainable Polymers (CHE-1901635) at the University of Minnesota. Parts of this work were carried out in the Characterization Facility at the University of Minnesota, which receives partial support from the NSF through the MRSEC program (DMR-2011401).

References

(1) Schneiderman, D. K.; Hillmyer, M. A. 50th Anniversary Perspective: There Is a Great Future in Sustainable Polymers. *Macromolecules* **2017**, *50* (10), 3733–3749. https://doi.org/10.1021/acs.macromol.7b00293.

(2) Tokiwa, Y.; Calabia, B. P.; Ugwu, C. U.; Aiba, S. Biodegradability of Plastics Bio-Plastics. *Int. J. Mol. Sci.* **2009**, *10*, 3722–3742. https://doi.org/10.3390/ijms10093722.

(3) Sodergard, A.; Stolt, M. Properties of Polylactic Acid Fiber Based Polymers and Their Correlation with Composition. *Prog. Polym. Sci.* **2002**, *27*, 1123–1163.

(4) Garlotta, D. A Literature Review of Poly (Lactic Acid). *J. Polym. Environ.* **2001**, *9* (2), 63–84.

(5) Datta, R.; Henry, M. Review Lactic Acid: Recent Advances in Products, Processes and Technologies – a Review. *J. Chem. Technol. Biotechnol.* **2006**, *81*, 1110–1129. https://doi.org/10.1002/jctb.

(6) Li, X.; Kang, H.; Shen, J.; Zhang, L.; Nishi, T.; Ito, K.; Zhao, C.; Coates, P. Highly Toughened Polylactide with Novel Sliding Graft Copolymer by in Situ Reactive Compatibilization, Crosslinking and Chain Extension. *Polymer (Guildf).* **2014**, *55* (16),

4313–4323. https://doi.org/10.1016/j.polymer.2014.06.045.

(7) Liu, H.; Zhang, J. Research Progress in Toughening Modification of Poly(Lactic Acid). *J. Polym. Sci. Part B Polym. Phys.* **2011**, *49* (15), 1051–1083. https://doi.org/10.1002/polb.22283.

(8) Anderson, K. S.; Schreck, K. M.; Hillmyer, M. A. Toughening Polylactide. *Polym. Rev.* **2008**, *48* (1), 85–108. https://doi.org/10.1080/15583720701834216.

(9) Zhao, X.; Hu, H.; Wang, X.; Yu, X.; Zhou, W.; Peng, S. Super Tough Poly(Lactic Acid) Blends: A Comprehensive Review. *RSC Adv.* **2020**, *10* (22), 13316–13368. https://doi.org/10.1039/d0ra01801e.

(10) Bucknall, C. B. *Toughened Plastics*; Springer, 1977. https://doi.org/10.1007/978-94-017-5349-4.

(11) Adhikari, R.; Michler, G. H. Influence of Molecular Architecture on Morphology and Micromechanical Behavior of Styrene/Butadiene Block Copolymer Systems. *Prog. Polym. Sci.* **2004**, *29* (9), 949–986. https://doi.org/10.1016/j.progpolymsci.2004.06.002.

(12) Sinclair, R. G. The Case for Polylactic Acid as a Commodity Packaging Plastic. *J. Macromol. Sci. - Pure Appl. Chem.* **1996**, *33* (5), 585–597. https://doi.org/10.1080/10601329608010880.

(13) Labrecque, L. V.; Kumar, R. A.; Davé, V.; Gross, R. A.; Mccarthy, S. P. Citrate Esters as Plasticizers for Poly(Lactic Acid). *J. Appl. Polym. Sci.* **1997**, *66* (8), 1507–1513. https://doi.org/10.1002/(SICI)1097-4628(19971121)66:8<1507::AID-APP11>3.0.CO;2-0.

(14) Baiardo, M.; Frisoni, G.; Scandola, M.; Rimelen, M.; Lips, D.; Ruffieux, K.; Wintermantel, E. Thermal and Mechanical Properties of Plasticized Poly(L-Lactic Acid). *J. Appl. Polym. Sci.* **2003**, *90* (7), 1731–1738. https://doi.org/10.1002/app.12549.

(15) Nijenhuis, A. J.; Colstee, E.; Grijpma, D. W.; Pennings, A. J. High Molecular Weight Poly(L-Lactide) and Poly(Ethylene Oxide) Blends: Thermal Characterization and Physical Properties. *Polymer (Guildf).* **1996**, *37* (26), 5849–5857. https://doi.org/10.1016/S0032-3861(96)00455-7.

(16) Gajria, A. M.; Davé, V.; Gross, R. A.; McCarthy, S. P. Miscibility and Biodegradability of Blends of Poly(Lactic Acid) and Poly(Vinyl Acetate). *Polymer (Guildf).* **1996**, *37* (3), 437–444. https://doi.org/10.1016/0032-3861(96)82913-2.

(17) Ljungberg, N.; Wesslén, B. Preparation and Properties of Plasticized Poly(Lactic Acid) Films. *Biomacromolecules* **2005**, *6* (3), 1789–1796. https://doi.org/10.1021/bm050098f.

(18) Anderson, K. S.; Lim, S. H.; Hillmyer, M. A. Toughening of Polylactide by Melt Blending with Linear Low-Density Polyethylene. *J. Appl. Polym. Sci.* **2003**, *89* (14), 3757–3768. https://doi.org/10.1002/app.12462.

(19) Hiljanen-Vainio, M.; Varpomaa, P.; Seppälä, J.; Törmälä, P. Modification of Poly(L-Lactides) by Blending: Mechanical and Hydrolytic Behavior. *Macromol. Chem. Phys.* **1996**, *197* (4), 1503–1523. https://doi.org/10.1002/macp.1996.021970427.

(20) Jiang, L.; Wolcott, M. P.; Zhang, J. Study of Biodegradable Polylactide/Poly(Butylene Adipate-Co-Terephthalate) Blends. *Biomacromolecules* **2006**, *7* (1), 199–207. https://doi.org/10.1021/bm050581q.

(21) Wu, N.; Zhang, H.; Fu, G. Super-Tough Poly(Lactide) Thermoplastic Vulcanizates Based on Modified Natural Rubber. *ACS Sustain. Chem. Eng.* **2017**, *5* (1), 78–84. https://doi.org/10.1021/acssuschemeng.6b02197.

(22) Ishida, S.; Nagasaki, R.; Chino, K.; Dong, T.; Inoue, Y. Toughening of Poly(L-Lactide) by Melt Blending with Rubbers. *J. Appl. Polym. Sci.* **2009**, *113*, 558–566.

https://doi.org/10.1002/app.

(23) Di Lorenzo, M. L. Poly(l-Lactic Acid)/Poly(Butylene Succinate) Biobased Biodegradable Blends. *Polym. Rev.* **2020**. https://doi.org/10.1080/15583724.2020.1850475.

(24) Li, T.; Zhang, J.; Schneiderman, D. K.; Francis, L. F.; Bates, F. S. Toughening Glassy Poly(Lactide) with Block Copolymer Micelles. *ACS Macro Lett.* **2016**, *5* (3), 359–364. https://doi.org/10.1021/acsmacrolett.6b00063.

(25) Jiang, H.; Ding, Y.; Liu, J.; Alagarsamy, A.; Pan, L.; Song, D.; Zhang, K.; Li, Y. Supertough Poly(Lactic Acid) and Sustainable Elastomer Blends Compatibilized by PLLA- b -PMMA Block Copolymers as Effective A- b -C-Type Compatibilizers . *Ind. Eng. Chem. Res.* **2020**, *59* (31), 13956–13968. https://doi.org/10.1021/acs.iecr.0c00988.

(26) McCutcheon, C. J.; Zhao, B.; Jin, K.; Bates, F. S.; Ellison, C. J. Crazing Mechanism and Physical Aging of Poly(Lactide) Toughened with Poly(Ethylene Oxide)-Block-Poly(Butylene Oxide) Diblock Copolymers. *Macromolecules* **2020**, *53* (22), 10163–10178. https://doi.org/10.1021/acs.macromol.0c01759.

(27) Pluta, M.; Piorkowska, E. Tough Crystalline Blends of Polylactide with Block Copolymers of Ethylene Glycol and Propylene Glycol. *Polym. Test.* **2015**, *46*, 79–87. https://doi.org/10.1016/j.polymertesting.2015.06.014.

(28) Chen, S. C.; Wang, Y. Z.; Yang, D. D.; Wu, C.; Wu, G. Toughening of Polylactide with High Tensile Strength via Constructing an Integrative Physical Crosslinking Network Based on Ionic Interactions. *Macromolecules* **2021**, *54*, 291–301. https://doi.org/10.1021/acs.macromol.0c02181.

(29) Leibler, L. Nanostructured Plastics: Joys of Self-Assembling. *Prog. Polym. Sci.* **2005**, *30* (8–9), 898–914. https://doi.org/10.1016/j.progpolymsci.2005.06.007.

(30) Xu, J.; Howard, M. J.; Mittal, V.; Bates, F. S. Block Copolymer Micelle Toughened Isotactic Polypropylene. *Macromolecules* **2017**, *50* (17), 6421–6432. https://doi.org/10.1021/acs.macromol.7b01656.

(31) Jing, F.; Hillmyer, M. A. A Bifunctional Monomer Derived from Lactide for Toughening Polylactide. *J. Am. Chem. Soc.* **2008**, *130* (42), 13826–13827. https://doi.org/10.1021/ja804357u.

(32) Zhang, J.; Schneiderman, D. K.; Li, T.; Hillmyer, M. A.; Bates, F. S. Design of Graft Block Polymer Thermoplastics. *Macromolecules* **2016**, *49* (23), 9108–9118. https://doi.org/10.1021/acs.macromol.6b02033.

(33) Zhang, J.; Li, T.; Mannion, A. M.; Schneiderman, D. K.; Hillmyer, M. A.; Bates, F. S. Tough and Sustainable Graft Block Copolymer Thermoplastics. *ACS Macro Lett.* **2016**, *5* (3), 407–412. https://doi.org/10.1021/acsmacrolett.6b00091.

(34) Haugan, I. N.; Lee, B.; Maher, M. J.; Zografos, A.; Schibur, H. J.; Jones, S. D.; Hillmyer, M. A.; Bates, F. S. Physical Aging of Polylactide-Based Graft Block Polymers. *Macromolecules* **2019**, *52* (22), 8878–8894. https://doi.org/10.1021/acs.macromol.9b01434.

(35) Michalski, A.; Brzezinski, M.; Lapienis, G.; Biela, T. Star-Shaped and Branched Polylactides: Synthesis, Characterization, and Properties. *Prog. Polym. Sci.* **2019**, *89*, 159–212. https://doi.org/10.1016/j.progpolymsci.2018.10.004.

(36) Deng, Y.; Zhang, S.; Lu, G.; Huang, X. Constructing Well-Defined Star Graft Copolymers. *Polym. Chem.* **2013**, *4* (5), 1289–1299. https://doi.org/10.1039/c2py20622f.

(37) Yang, X.; Liu, S.; Yu, E.; Wei, Z. Toughening of Poly(l -Lactide) with Branched Polycaprolactone: Effect of Chain Length. *ACS Omega* **2020**, *5* (45), 29284–29291.

https://doi.org/10.1021/acsomega.0c04070.

(38) Dandan Doganci, M.; Aynali, F.; Doganci, E.; Ozkoc, G. Mechanical, Thermal and Morphological Properties of Poly(Lactic Acid) by Using Star-Shaped Poly(ε-Caprolactone) with POSS Core. *Eur. Polym. J.* **2019**, *121* (August), 109316. https://doi.org/10.1016/j.eurpolymj.2019.109316.

(39) Koning, C.; Van Duin, M.; Pagnoulle, C.; Jerome, R. Strategies for Compatibilization of Polymer Blends. *Prog. Polym. Sci.* **1998**, *23* (4), 707–757. https://doi.org/10.1016/S0079-6700(97)00054-3.

(40) Sookprasert, P.; Hinchiranan, N. Morphology, Mechanical and Thermal Properties of Poly(Lactic Acid) (PLA)/Natural Rubber (NR) Blends Compatibilized by NR-Graft-PLA. *J. Mater. Res.* **2017**, *32* (4), 788–800. https://doi.org/10.1557/jmr.2017.9.

(41) Watts, A.; Kurokawa, N.; Hillmyer, M. A. Strong, Resilient, and Sustainable Aliphatic Polyester Thermoplastic Elastomers. *Biomacromolecules* **2017**, *18* (6), 1845–1854. https://doi.org/10.1021/acs.biomac.7b00283.

(42) Lundberg, D. J.; Lundberg, D. J.; Hillmyer, M. A.; Dauenhauer, P. J. Techno-Economic Analysis of a Chemical Process to Manufacture Methyl-Îμ -Caprolactone from Cresols. *ACS Sustain. Chem. Eng.* **2018**, *6* (11), 15316–15324. https://doi.org/10.1021/acssuschemeng.8b03774.

(43) De Hoe, G. X.; Zumstein, M. T.; Tiegs, B. J.; Brutman, J. P.; McNeill, K.; Sander, M.; Coates, G. W.; Hillmyer, M. A. Sustainable Polyester Elastomers from Lactones: Synthesis, Properties, and Enzymatic Hydrolyzability. *J. Am. Chem. Soc.* **2018**, *140* (3), 963–973. https://doi.org/10.1021/jacs.7b10173.

(44) Maher, M. J.; Schibur, H. J.; Bates, F. S. When Convergent Syntheses of Graft Block

Copolymers Diverge: The Treachery of Chemical Images. *J. Polym. Sci. Part A Polym. Chem.* **2017**, *55* (18), 3097–3104. https://doi.org/10.1002/pola.28660.

(45) Dorgan, J. R.; Williams, J. S.; Lewis, D. N. Melt Rheology of Poly(Lactic Acid): Entanglement and Chain Architecture Effects. *J. Rheol. (N. Y. N. Y).* **1999**, *43* (5), 1141–1155. https://doi.org/10.1122/1.551041.

(46) Puig, J.; Ceolín, M.; Williams, R. J. J.; Schroeder, W. F.; Zucchi, I. A. Controlling the Generation of Bilayer and Multilayer Vesicles in Block Copolymer/Epoxy Blends by a Slow Photopolymerization Process. *Soft Matter* **2017**, *13* (40), 7341–7351. https://doi.org/10.1039/c7sm01660c.

(47) Gu, D.; Bongard, H.; Deng, Y.; Feng, D.; Wu, Z.; Fang, Y.; Mao, J.; Tu, B.; Schüth, F.; Zhao, D. An Aqueous Emulsion Route to Synthesize Mesoporous Carbon Vesicles and Their Nanocomposites. *Adv. Mater.* **2010**, *22* (7), 833–837. https://doi.org/10.1002/adma.200902550.

(48) Lee, B.; Onbulak, S.; Xu, Y.; Topolkaraev, V.; McEneany, R.; Bates, F.; Hillmyer, M. Investigation of Micromechanical Behavior and Voiding of Polyethylene Terephthalate/Polyethylene- Stat-Methyl Acrylate Blends during Tensile Deformation. *Ind. Eng. Chem. Res.* **2019**, *58* (16), 6402–6412. https://doi.org/10.1021/acs.iecr.8b06362.

(49) Theryo, G.; Jing, F.; Pitet, L. M.; Hillmyer, M. A. Tough Polylactide Graft Copolymers. *Macromolecules* **2010**, *43* (18), 7394–7397. https://doi.org/10.1021/ma101155p.